Songklanakarin J. Sci. Technol.
45 (1), 80–87, Jan. – Feb. 2023

http://www.sjst.psu.ac.th

Original Article

Flow of a Casson fluid with heat transfer over a shrinking sheet and its dual solutions

Debasish Dey and Rupjyoti Borah*

Department of Mathematics, Dibrugarh University, Dibrugarh, Assam, 786004 India

Received: 14 June 2021; Revised: 27 October 2022; Accepted: 6 December 2022

Abstract

An effort has been made to examine the dual solutions of boundary layer flow of the Casson fluid over a shrinking sheet, with the effects of Joule heating and power-law heat flux. A homogeneous magnetic field is implemented in the system along a direction normal to the flow. Appropriate similarity transformations are employed to reformulate the governing equations of the present problem into a solvable set and the solution uses the three-stage Lobatto IIIa method in a developed numerical bvp4c code in MATLAB. Due to the shrinking surface, some disturbances impact the flow, which has two solutions: one that is stable and another that is unstable. Graphical results are shown to assess the velocity and temperature fields. A stability analysis is executed to characterize the stable and physically attainable solution. It is perceived that the Casson fluid parameter contributes to speed and temperature of the fluid in a time-independent case. Also, it controls the motion as well as the temperature of the fluid in the time-dependent case.

Keywords: magnetohydrodynamics, Casson fluid, dual solutions, heat transfer, joule heating, stability analysis

1. Introduction

Recently, there non-Newtonian fluids have been applied in various areas of engineering, sciences, and industrial processes. There is a huge amount of research on boundary layer flow of non-Newtonian fluids, with effects of both thermal and mass diffusivity becoming recently available. Non-Newtonian flows remain a special challenge to engineers, physicists, and mathematicians, due to their complexity despite the vast significance of these fluid in applications. The Casson fluids are a subclass of non-Newtonian fluids, with particular significance in food processing, metallurgy, drilling operations, bio-engineering, etc. Some important examples of this fluid type are honey, concentrated fruit juices, blood, and tomato sauce. This type of fluid has a yield stress and its characteristics dependent on both shear stress and yield stress. If the applied shear stress on the fluid is lesser than the yield stress, then this type of fluid has an infinite viscosity and behaves like a solid. However, it behaves like a liquid when the shear stress exceeds the yield stress. Amilmohamadi, Akram, and Sadeghy (2016), Zaib, Bhattacharyya, Uddin, and Shafie (2016), Tamoor, Waqas, Khan, Alsaedi, and Hayat (2017), Maraj, Faizan, and Shaiq (2019) and Shah, Kumam, and Deebani (2020) have given physical significance to the Casson fluid flow in different physical areas of different geometries. Oke, Mutuku, Kimathi, and Animasaun (2020) have investigated the Casson fluid under the action of Coriolis forces, and its importance in different fields with rotating non-uniform surfaces. Alghamdi *et al.* (2020) have investigated the boundary-layer flow of Casson hybrid nanofluid streaming above an elongating surface. They concluded that this fluid model with the hybrid nanoparticles is very important for the enhancement of thermal conductivity, and this is a key requirement for the modern industries. Nandeppanavar, M.C., and Raveendra (2021) have examined the simultaneous influence of both thermal and mass transfer in Casson fluid flow with variable thermal radiation.

The flow due to the shrinking surface along with the effects of both thermal and mass diffusivity has received a great deal of interest in engineering sciences, and industrial processes of many areas. Some examples are wire drawing, extrusion, metal spinning and hot rolling, etc. Both heat and mass transfer over a stretching/shrinking surface occur in

*Corresponding author
Email address: debasish41092@gmail.com

annealing and thickening of a copper wire. The boundary-layer flow over contracting/moving surface was first introduced by Crane (1970). The researchers Krishna, Reddy, and Makinde (2018), Sarkar *et al.* (2019), Anuradha and Punithavalli (2019), Vaidya *et al*. (2020), Dey and Chutia (2021), Dey and Hazarika (2021) and Dey, Borah, and Mahanta (2021), have discussed the boundary layer flow of different fluid models due to stretching/shrinking type surfaces and their importance in different areas. They have also investigated the thermal transfer in the fluid flow for its importance in different fields. In the recent times, the Joule heating and heat source effect and magnetohydrodynamics on this present model are found in important applications in different physical areas. Many researchers, Hayat, Shafiq, and Alsaedi (2014), Khan, Khan, Irfan, and Alshomrani (2017), Saidulu and Lakshmi (2017) and Ibrahim, Kumar, Lorenzini, and Lorenzini (2019) have analysed the consequences of Joule heating and heat source effects on a variety of surfaces. Adnan, Arifin, Bachok, and Ali (2019) have discussed the importance of the shrinking surface during the fluid streaming above. The effects of the magnetic field during fluid flow of this type has many industrial applications in MHD (magneto-hydrodynamics) pumps and MHD generators etc. Zehra *et al*. (2021) have investigated the Casson nanofluid flow over a curved stretching/shrinking channel with homogeneous magnetic field. Jamshed *et al*. (2021) have explored the ideas of the magnetized fluid streaming above shrinking/stretching surfaces by employing the Casson fluid model.

Markin (1980) introduced the dual type solutions and found that the upper branch, i.e., the time dependent solution, is unstable. After that, a huge amount of literature on boundary layer flows and their dual solutions has emerged. Many researchers, Najib, Bachok, and Arifin (2017), Ahmed, Siddique, and Sagheer (2018), Salleh, Bachok, Arifin, Ali, and Pop (2018), Dey and Borah (2020) and Mishra, Hussain, Seth, and Makinde (2020) have analysed the dual solutions and their stability. They have found two types of solutions and interpreted that the time independent solution is stable in nature and physically achievable. Dey and Borah (2021) have investigated the numerical solutions of the two-fold solutions of the fluid flow caused due to an elongating surface under the action of both thermal and mass transmission by considering the second-grade fluid. Dey, Makinde, and Borah (2022) have scrutinized the nature of the dual solutions and their occurrence during the flow of the fluid under the effects of both thermal and mass transfer over a stretching/shrinking surface. Dey, Borah, and Khound (2022) have studied the dual solutions and their stability for Casson fluid flow over an elongating sheet. They found that the first solution, which is for the time-independent case, is stable and physically tractable. All the above cited literature has studied the impacts of a magnetic field on various fluid flows caused by stretching/shrinking of surfaces.

In fluid mechanics, all the flow problems are elaborated based on some physical principles of conservation. These physical laws give the governing mathematical equations that describe the patterns of motion, temperature, as well as mass transfer in the fluid. These equations are highly non-linear, so only few analytical solutions are known in special cases. In this study, we adopted the three-stage Lobatto IIIa formula [referring to Shampine, Kierzenka, and Reichelt (2000)] for solving the boundary value problems by developing a numerical bvp4c code in MATLAB. Many researchers such as Dey and Borah (2020, 2021) and Dey, Hazarika, Borah (2021) have applied the MATLAB routine bvp4c solver scheme in their studies.

The objective of this study was to explore the nature of dual solutions of the Casson fluid flow due to contracting sheet with the Joule heating and heat source. A constant magnetic field is applied normal to the flow direction. Adopting suitable similarity transformations, a third order differential equation corresponding to flow equation and a second order equation corresponding to heat transfer equation are developed. The numerical calculations and visualization are carried out for different flow parameters by using MATLAB built-in bvp4c solver. Numerical results have been confirmed by comparison against the previous results of Jaber (2016) for a certain case, with excellent agreement. The nature of dual solutions and their stability for the Casson fluid flow due to contracting surface are the novelty of this work.

2. Formulation of the Problem

The following assumptions were made to formulate this present problem in terms of mathematical equations. The flow diagram of this problem is shown in Figure (1).

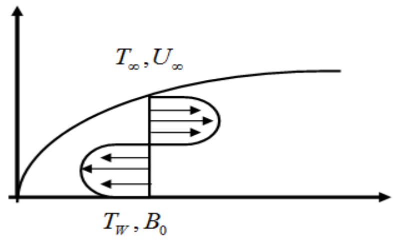

Figure 1. Flow diagram

(i) 2D, time-independent and incompressible flow of Casson fluid over a shrinking sheet,
(ii) a constant magnetic field of strength (B_0) is applied in the vertical direction over the sheet,
(iii) the flow is induced by (a) inertial forces, (b) viscous forces, (c) pressure gradient and (d) Lorentz forces,
(iv) the contracting sheet is characterized by the velocity of the fluid $u = -cx$, where the constant $c > 0$ represents the shrinkage of the sheet at $y = 0$ and
(v) in heat transfer, the flow is maintained by both free convection and conduction, heat generation, dissipation of energy and Joule heating with prescribed wall temperature $T_W(x) = T_\infty + Bx^2\sqrt{\upsilon c^{-1}}$
(vi) the constitutive equation of the present fluid model [referring to Lund, Omar, Khan, Baleanu, and Nisar (2020)] which represents the isotropic and incompressible progression of the fluid is stated as:

$$\tau_{ij} = \begin{cases} 2\left(\mu_B + \dfrac{P_y}{\sqrt{2\pi}}\right)e_{ij}, & \pi > \pi_c \\ 2\left(\mu_B + \dfrac{P_y}{\sqrt{2\pi_c}}\right)e_{ij}, & \pi < \pi_c \end{cases}$$

where, the plastic dynamic viscosity of this fluid model is determined by μ_B, $\pi = e_{ij}e_{ij}$ is the $(i, j)^{th}$ deformation rate of the fluid, π_c the critical value of the deformation rate and the yield stress of the fluid is denoted by P_y.

(vii) One of the most important forces in the present fluid model streaming above a contracting surface is the Lorentz force that can be expressed as

$$\vec{F} = q\,\vec{v}\times\vec{B}.$$

where, $\vec{B} = B_0 y$ is the magnetic field that applied in the direction normal to the flow and q the charge and $\vec{v}$ the velocity vector.

Following boundary layer theory, the foremost equations of this study are:

$$\frac{\partial u}{\partial x}+\frac{\partial v}{\partial y}=0, \tag{1}$$

$$u\frac{\partial u}{\partial x}+v\frac{\partial u}{\partial y}=\upsilon\left(1+\frac{1}{\beta}\right)\frac{\partial^2 u}{\partial y^2}-\frac{\sigma B_0^{\,2}}{\rho}u, \tag{2}$$

$$u\frac{\partial T}{\partial x}+v\frac{\partial T}{\partial y}=\frac{k}{\rho C_P}\frac{\partial^2 T}{\partial y^2}+\frac{Q*}{\rho C_P}\left(T-T_\infty\right)-\frac{\mu_\beta}{\rho C_P}\left(1+\frac{1}{\beta}\right)\left(\frac{\partial u}{\partial y}\right)^2+\frac{\sigma B_0^{\,2}}{\rho C_P}u^2. \tag{3}$$

The conditions at the surface are:

$$\begin{aligned} &y=0: u=cx, v=-v_0, \frac{\partial T}{\partial y}=Bx^2;\\ &y\to\infty: u\to 0, v\to 0, T\to T_\infty. \end{aligned} \tag{4}$$

where, c is a constant and its negative value indicates that there is shrinkage of the sheet at the surface.

The following similarity transformations are employed to remodel the equations [(1)-(3)].

$$u=cxf\,'(\eta), v=-\sqrt{\upsilon c}\,f(\eta), \eta=\sqrt{c\upsilon^{-1}}\,y, \theta(\eta)=\frac{T-T_\infty}{T_W-T_\infty}. \tag{5}$$

The equation (1) then is clearly satisfied, and the other two equations get the following forms:

$$\left(1+\frac{1}{\beta}\right)f\,'''+ff\,''-f\,'^2-Mf\,'=0, \tag{6}$$

$$\theta''+\Pr f\theta'-2\Pr f\,'\theta-\Pr H\theta+\Pr Ec\left(1+\frac{1}{\beta}\right)f\,''^2+EcJf\,'^2=0. \tag{7}$$

The boundary condition (4) becomes:

$$\begin{aligned} &\eta=0: f(\eta)=s, f\,'(\eta)=-1, \theta'(\eta)=1;\\ &\eta\to\infty: f\,'(\eta)\to 0; \theta(\eta)\to 0. \end{aligned} \tag{8}$$

The flow parameters that are involved in this investigation are defined in the following way:

$$s=\frac{v_0}{\sqrt{c\eta}}, \Pr=\frac{\mu C_P}{k}, M=\frac{\sigma B_0^{\,2}}{\rho c}, Ec=\frac{c\sqrt{c}}{BC_P\sqrt{\upsilon}}, J=\frac{\sigma B_0^{\,2}\mu C_P}{\rho^2 k}, H=\frac{\upsilon Q*}{C_P c\rho}\ \&\ \beta=\frac{\mu_B\sqrt{2\pi_c}}{P_y}.$$

The following physical quantities are observed in this study that are very important in several physical areas such as engineering sciences and industrial processes. The skin friction coefficient (C_f) and the Nusselt number (rate of heat transfer) (N_u) are defined in the following way:

$$C_f=\frac{\mu\left(1+\frac{1}{\beta}\right)}{\rho u_w^{\,2}}\left(\frac{\partial u}{\partial y}\right)_{y=0}\ \&\ Nu=-\frac{x}{(T_w-T_\infty)}\left(\frac{\partial T}{\partial y}\right)_{y=0}. \tag{9}$$

Then we have,

$$C_f=\frac{\mu\left(1+\frac{1}{\beta}\right)x}{\rho\sqrt{\upsilon c}}f\,''(0)\ \&\ Nu=-Bx^3\theta'(0). \tag{10}$$

3. Flow Stability

To characterize the more stable and physically attainable solution, the time dependent governing equations are needed. So, we have considered the unsteady form of governing equations (2) and (3) by adding the terms $\frac{\partial u}{\partial t}$ & $\frac{\partial T}{\partial t}$ in (2) and (3) respectively. To solve the unsteady form of governing equations, the following new similarity transformations are employed:

$$u = cxf'(\eta,\tau), v = -\sqrt{\upsilon c}\, f(\eta,\tau), \eta = \sqrt{c\upsilon^{-1}}\, y, \theta(\eta,\tau) = \frac{T - T_\infty}{T_W - T_\infty} \;\&\; \tau = ct. \tag{11}$$

where t is the time. After applying equations (11) in the unsteady governing equations, we have achieved the following set of equations:

$$\left(1+\frac{1}{\beta}\right)\frac{\partial^3 f}{\partial \eta^3} + f(\eta,\tau)\frac{\partial^2 f}{\partial \eta^2} - \left(\frac{\partial f}{\partial \eta}\right)^2 - M\frac{\partial f}{\partial \eta} - \frac{\partial^2 f}{\partial \eta \partial \tau} = 0, \tag{12}$$

$$\frac{\partial^2 \theta}{\partial \eta^2} + \Pr f(\eta,\tau)\frac{\partial \theta}{\partial \eta} - 2\Pr\frac{\partial f}{\partial \eta}\theta(\eta,\tau) - H\theta(\eta,\tau) + \Pr Ec\left(1+\frac{1}{\beta}\right)\left(\frac{\partial^2 f}{\partial \eta^2}\right)^2 + EcJ\left(\frac{\partial f}{\partial \eta}\right)^2 - \Pr\frac{\partial \theta}{\partial \tau} = 0, \tag{13}$$

The pertinent boundary conditions are:

$$\begin{aligned} &\frac{\partial f}{\partial \eta}(0,\tau) = -1, f(0,\tau) = s, \frac{\partial \theta}{\partial \eta}(0,\tau) = 1; \\ &\frac{\partial f}{\partial \eta}(\infty,\tau) \to 0, \theta(\infty,\tau) \to 0. \end{aligned} \tag{14}$$

Following Markin (1980) and Weidman and Awaludin (2016), the following perturbed (separation of variables) equations are considered, which helps to simplify the equations (12) and (13) and transform them into linearized form.

$$\begin{aligned} &f(\eta,\tau) = f_0(\eta) + e^{-\lambda\tau}F(\eta,\tau), \theta(\eta,\tau) = \theta_0(\eta) + e^{-\lambda\tau}G(\eta,\tau), \\ &\phi(\eta,\tau) = \phi_0(\eta) + e^{-\lambda\tau}H(\eta,\tau). \end{aligned} \tag{15}$$

where, f_0 & θ_0 are the solutions of the time free equations and *F*&*G* are small relative to steady flow solutions; and λ is an unknown eigenvalue parameter. To obtain the steady flow solutions, we have to set $\tau \to 0$, which give $F = F_0 \;\&\; G = G_0$. Therefore, we have perceived the following set of linearized eigenvalue problems.

$$\left(1+\frac{1}{\beta}\right)F_0''' + \left(f_0 F_0'' + F_0 f_0''\right) - 2f_0' F_0' - MF_0' + \lambda F_0' = 0, \tag{16}$$

$$\begin{aligned} &G_0'' + \Pr\left(f_0 G_0' + F_0\theta_0'\right) - 2\Pr\left(f_0' G_0 + F_0'\theta_0\right) - HG_0 + 2\Pr Ec\left(1+\frac{1}{\beta}\right)f_0'' F_0'' + 2EcJ\Pr f_0' F_0' \\ &+ \Pr\lambda G_0 = 0, \end{aligned} \tag{17}$$

and the conditions at the surface become

$$F_0'(0) = 0, F_0(0) = 0, G_0'(0) = 0; F_0'(\infty) \to 0, G_0(\infty) \to 0. \tag{19}$$

Solving these equations, we get an infinite set of eigenvalues. Among these eigenvalues, the positive smallest eigenvalue represents an initial decay of disturbances to the flow and hence the flow will be stable by its nature. If the least eigenvalue is found to be negative, then an initial growth of disturbances happens in the flow, and hence the flow will be unstable. To evaluate the fixed eigenvalues, we have relaxed the boundary condition $F_0'(\infty) \to 0$ to the new boundary condition $F_0''(0) = 1$ [following Harish, Ingham, and Pop (2009) and Weidman and Awaludin (2016)].

4. Discussion of the Results

The "MATLAB built-in bvp4c solver" was adopted to work out this problem [following Shampine, Kierzenka, and Reichelt (2000), Dey and Hazarika (2020) and Dey and Chutia (2020)]. The dimensionless Prandtl number (Pr) was fixed to 0.72 throughout this investigation, which physically signifies higher thermal conductivity materials-air (Pr = 0.7 < 1, thermal diffusivity is greater than momentum diffusivity) [referring Salleh, Bachok, Arifin, Ali, and Pop (2010)]. The visualization of flow behaviours is done with the help of graphs for different values of flow parameters. Special highlights are given for the Casson fluid parameter (β) as its value $\beta \to \infty$ approaches the Newtonian fluid; along with heat source parameter (*H*) and Joule heating parameter (*J*).

4.1 Verification of the results

To validate our results, we have compared our numerical values of the shear stress at the surface for the steady Newtonian fluid $(\beta \rightarrow \infty)$ in the case of stretching sheet with the pioneer work of Jaber (2016). Table (1) shows a very good conformity of our results. This concordance gives confidence also to the other results.

The numerical values of smallest eigenvalue are given in Table 2. It is seen that the least eigenvalues for the steady flow solution are positive. The initial disturbances in the flow decay, consequently this being a stable steady flow solution. In the unsteady solutions, the smallest eigenvalues are found to be negative, allowing disturbances in the flow to grow and make it unstable.

Figures 2 and 3 illustrate the motion and temperature of the fluid for various values of the Casson fluid parameter (β). From Figure 2, it is perceived that increasing β accelerates the motion of the fluid in both the time-independent and the time-dependent cases. Generally, a larger β decelerates the motion of the fluid because it raises the plastic dynamic viscosity, but the opposite behaviour is observed for the flow here, and this happens only because of the special geometry (shrinking surface). From Figure 3, it is noted that the temperature of the fluid decreases with β. This can be physically understood as higher values of β enhance the resistance of the fluid and reduce the effects of yield stress on the fluid, and hence the temperature pattern gets slower in both cases. Further, it can be concluded that in the time-dependent case, the velocity and temperature of the fluid converge to its free stream region more quickly than in the time-independent case. Due to the magnetic field in the system, the speed of the motion in both the cases (steady and unsteady) accelerates [shown in Figure 4]. It can be physically reasoned that increasing the magnetic parameter reduces the effects of viscosity of the fluid at the surface, making the Lorentz force dominate, and hence speed of the fluid increases. From Figure 5, it is seen that both of the solutions

Table 2. Numerical values of smallest eigenvalues for a range of the suction parameter (s) when Pr = 0.72, Ec = 3, J = 1, H = 1, M = 2 & β = 0.2

s	Smallest eigenvalue	
	Steady solution	Unsteady solution
2.5	2.5000	-2.3380
2.6	2.6000	-2.1521
2.7	2.7000	-2.7426

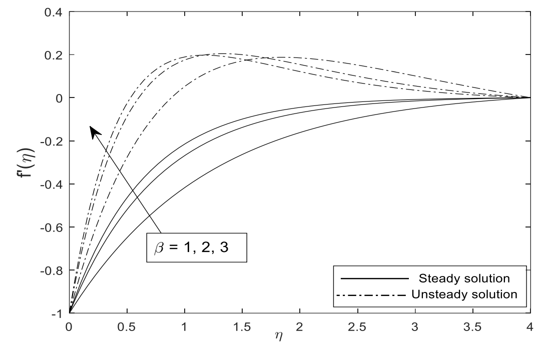

Figure 2. Impact of β on velocity distribution when Pr = 0.72, Ec = 3, J = 1, H = 1, M = 0.2 & s = 2.23

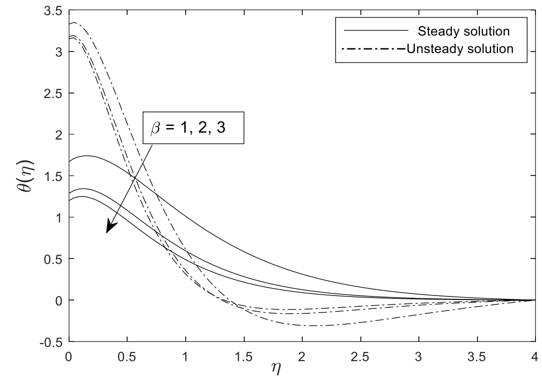

Figure 3. Impact of β on temperature field when Pr = 0.72, Ec = 3, J = 1, H = 1, M = 0.2 & s = 2.23

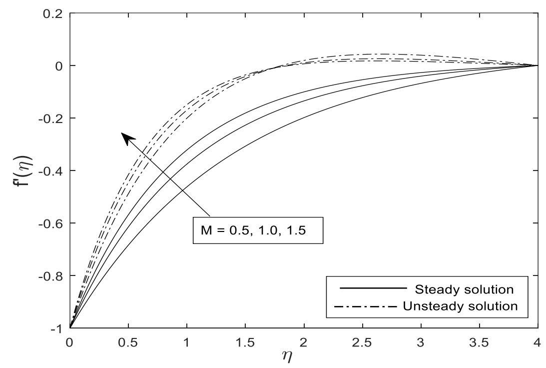

Figure 4. Impact of M on velocity field when Pr = 0.72, Ec = 3, J = 1, H = 1, M = 0.2, s = 2.23, & β = 0.2

Table 1. Numerical values of negative magnitude of skin-friction coefficient (-Cf) for various values of magnetic parameter (M) when Pr = 0.72, Ec = 3, J = 1, H = 1 & s = 1 in the case of Newtonian fluid and stretching sheet

M	Jaber (2016) result (shooting technique solutions)	Present results (bvp4c solution)	
		Steady solution	Unsteady solution
1.0	2.00007	2.0009	3.0311
3.0	2.56155	2.5616	3.1138
5.0	3.0	3.0	3.5311

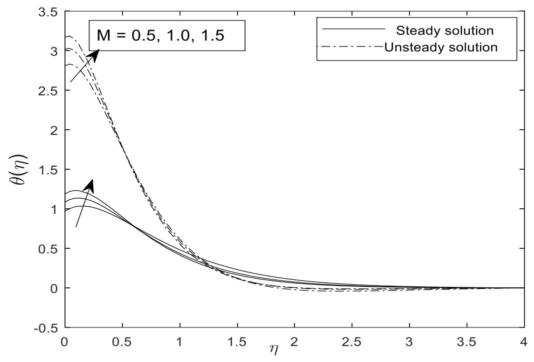

Figure 5. Impact of M on temperature field when Pr = 0.72, Ec = 3, J = 1, H = 1, M = 0.2, s = 2.23, & β = 0.2

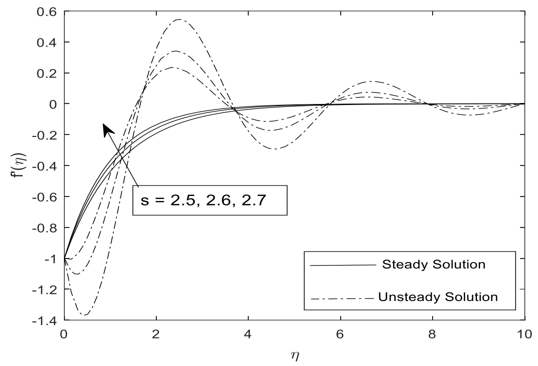

Figure 6. Impact of s on velocity field when Pr = 0.72, Ec = 3, J = 1, H = 1, M = 0.2, & β = 0.2

(steady and unsteady) of temperature distributions in the fluid increase near the surface of the sheet with M. It can be physically justified that enlarging M increases the magnetic force as well as friction of the fluid, and hence the temperature in the fluid in both cases increases. Also, maximum variation of the temperature field in the fluid is seen in the region $0 < \eta < 0.5$. Figure 6 is portrayed to investigate the nature of speed of the fluid due to effects of the suction parameter ($s > 0$). Increasing s increases the speed of the fluid in both the cases. Again, it is observed that the speed of the fluid during steady case is completely negative for various values of s. From this figure, it is also perceived that the speed of the fluid in time-dependent case oscillates in the region $2 < \eta < 10$ with increasing values of s. This happens only because of the additional fluid suction by the system and the shrinkage affect in opposite directions of the flow.

The consequences of heat source and Joule heating parameters on temperature distribution are plotted in Figures 7 and 8. From Figure 7, it is perceived that the temperature of the fluid decreases with H in both the time-independent and the time-dependent solutions. Generally, increasing H generates additional heat in the system and hence the temperature in the fluid tends to increase. However, the opposite is seen in this study because of the considered geometry, with shrinkage opposing the direction of flow. Also, it is seen that maximum temperature of the fluid is found in the vicinity of the surface and then gradually on going to its free stream region both the solutions become similar. The temperature change of the fluid during both steady and unsteady cases accelerates with more Joule heating (J). It is also noticed that the thermal boundary layer width in the steady solution is thinner than in the unsteady (time-dependent) solution. All the cases satisfy the far field boundary conditions asymptotically. Also, we have seen that both of the solutions exist within a certain region of the similarity variables η. Again, the steady solution is in the vicinity of the surface and converges to its free stream region quicker than the unsteady solutions, so the steady solution is more realizable than the unsteady solution.

5. Conclusions

In this study, we have investigated the two-fold solutions of the thermally stratified Casson fluid streaming above a contracting surface under the influence of magnetic

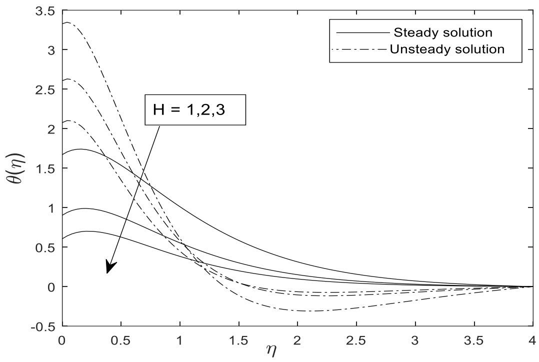

Figure 7. Impact of H on temperature field when Pr = 0.72, Ec = 3, J = 1, s = 2.23, M = 0.2, & β = 0.2

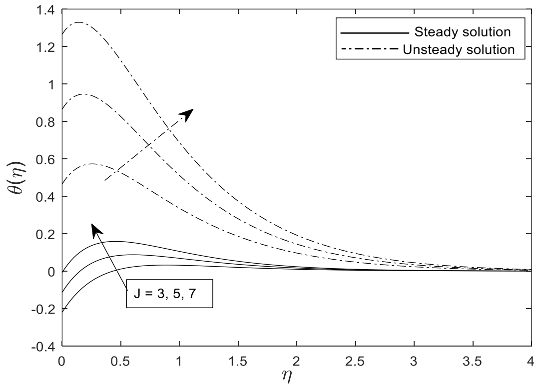

Figure 8. Impact of J on temperature field when Pr = 0.72, Ec = 3, H = 1, s = 2.23, M = 0.2, & β = 0.2

field. The pertinent flow parameters discussed in the result section of this study have multiple applications in diverse physical areas. Again, the considered fluid model is one of the most important in the recent research trends. The scientists and industrialists may use this fluid model under the influence of different factors that interact with flows, such as magnetic field, Joule heating, heat source, and suction/injection for achieving more benefits. The following are the key observations made in this study:

- All the profiles satisfy the far-field boundary conditions asymptotically and dual type solutions exist in a certain region of the similarity variables η.

- From the stability point of view, the steady flow solutions are stable and the unsteady flow solutions are unstable.
- The Casson fluid parameter has major significance to development of the speed of the fluid, as well as to control of the temperature of the fluid, which can save the system from damage.
- The magnetic field contributed to the motion of the fluid in both cases (time-independent and time-dependent). Again, increasing the magnetic field develops the temperature field of the fluid.
- The Joule heating contributes to the entire temperature field of the system.
- We can control the temperature of the fluid by utilizing the heat source.

The suction of the fluid in the system affects the motion of the fluid in both steady and unsteady cases.

Nomenclature

C	constant
B	constant
$f'(\eta)$	dimensionless velocity
Ec	Eckert number
H	heat source parameter
Q^*	heat generation parameter
J	Joule heating parameter
B_0	magnetic field (T)
M	Magnetic parameter
Nu	Nusselt number
Pr	Prandtl number
u	rate of displacement along x-directions (m/s)
v	rate of displacement along y-directions (m/s)
C_P	specific heat at constant pressure
V_0	suction/injection parameter
s	suction/injection parameter
C_f	skin friction coefficient
T	temperature of the fluid (K)
t	time variable (s)
k	thermal conductivity (m^2/s)
P_y	yield stress of the fluid (MPa)

Greek symbols:

β	Casson fluid parameter
ρ	density (kg/m^3)
τ	dimensionless time variable
$\theta(\eta)$	dimensionless temperature field
σ	electric density of the fluid (s/m)
υ	kinematic viscosity (m^2/s)
μ_β	plastic dynamic viscosity (pa.s)
η	similarity variable
ψ	stream function
λ	unknown eigen-value parameter

Suffix:

ω	at wall
∞	at free stream region"

References

Adnan, N. S. M., Arifin, N. M., Bachok, N. & Ali, F. M. (2019). Stability analysis of MHD flow and heat transfer passing a permeable exponentially shrinking Sheet with partial slip and thermal radiation. *CFD Letters*, *12*, 34-42.

Ahmed, A., Siddique, J. I. & Sagheer, M. (2018). Dual solutions in a boundary layer flow of a power law fluid over a moving permeable flat plate with thermal radiation, viscous dissipation and heat generation/absorption. *Fluids*, *3*(1).

Alghamdi, W., Gul, T., Nullah, M., Rehman, A., Nasir, S., Saeed, A. & Bonyah, E. (2020). Boundary layer stagnation point flow of the casson hybrid nanofluid over an unsteady stretching surface. *AIP Advances*, *11*, 015016.

Amlimohamadi, H., Akram , M. & Sadeghy, K. (2016). Flow of a casson fluid through a locally-constricted porous channel: a numerical study. *Korea Australia Rheology Journal*, *28*(2),129–137.

Anuradha, S. & Punithavalli, R. (2019). MHD boundary layer flow of a steady micro polar fluid along a stretching sheet with binary chemical reaction. *International Journal of Applied Engineering Research*, *14*(2), 440–446.

Crane, L. J. (1970). Flow past a stretching plate. *Zeitschrift für Angewandte Mathematik und Physik ZAMP*, *21*(4), 645–647.

Dey, D. & Borah, R. (2020). Dual solutions of boundary layer flow with heat and mass transfers over an exponentially shrinking cylinder: stability analysis. *Latin American Applied Research*, *50*(4), 247–253.

Dey, D. & Hazarika, M. (2020). Entropy generation of hydro-magnetic stagnation point flow of micropolar fluid with energy transfer under the effect of uniform suction / injection. *Latin American Applied Research*, *50*(3), 209–214.

Dey, D. & Chutia, B. (2020). Dusty nanofluid flow with bioconvection past a vertical stretching surface. *Journal of King Saud University- Engineering Sciences*. doi:10.1016/j.jksues.2020.11.001

Dey, D. & Borah, R. (2021). Stability analysis on dual solutions of second-grade fluid flow with heat and mass transfers over a stretching sheet. *International Journal of Thermofluid Science and Technology*, *8*(2), 080203.

Dey, D. & Chutia, B. (2021). Modelling of multi-phase fluid flow with volume fraction past a permeable stretching vertical cylinder and its numerical study. *Latin American Applied Research*, *51*(3), 165-171.

Dey, D., Hazarika, M. & Borah, R. (2021). Entropy generation analysis of magnetized micropolar fluid streaming above an exponentially extending plane. *Latin American Applied Research*, *51*(4), 255-260.

Dey, D. & Hazarika, M. (2021). Second law analysis of pseudo-plastic nanofluid stream past a stretching sheet with a sliding consequence. *Heat Transfer*, 1-15.

Dey, D., Makinde, O. D. & Borah, R. (2022). Analysis of dual solutions in MHD fluid flow with heat and mass transfer past an exponentially stretching/shrinking surface in a porous medium. *International Journal of Applied and Computational Mathematics, 8*(66). doi:10.1007/s40819-022-01268-7.

Dey, D., Borah, R. & Khound, A. S. (2022). Stability analysis on dual solutions of MHD Casson fluid flow with thermal and chemical reaction over a permeable elongating sheet. *Heat Transfer, 51*(4), 3401-3417.

Hayat, T., Shafiq, A. & Alsaedi, A. (2014). Effect of joule heating and thermal radiation in flow of third grade fluid over radiative surface. *PLoS One, 9*(1), 1–12.

Harish, S. D., Ingham, D. B. & Pop. I, (2009). Mixed convection boundary layer flow near the stagnation point on a vertical surface in a porous medium: Brinkman model with slip. *Transport Porous Media, 77, 267-285.*

Ibrahim, S. M., Kumar, P. V., Lorenzini, G. & Lorenzini, E. (2019). Influence of joule heating and heat source on radiative MHD flow over a stretching porous sheet with power-law heat flux. *Journal of Engineering Thermophysics, 28*(3), 332–344.

Jaber, K. K. (2016). Joule heating and viscous dissipation on effects on MHD flow over a stretching porous sheet subjected to power law heat flux in presence of heat source. *Open Journal of Fluid Dynamics*, *6*(3), 156–165.

Jamshed, W., Devi S, S. U., Goodarzi, M., Prakash, M., Nisar, K.S., Zakarya, M. & Abdel-Aty, A. H. (2021). Evaluating the unsteady casson nanofluid over a stretching sheet with solar thermal radiation: an optimal case study. *Case Studies in Thermal Engineering, 26*, 101160.

Khan, W. A., Khan, M., Irfan, M. & Alshomrani, A. S. (2017). Impact of melting heat transfer and nonlinear radiative heat flux mechanisms for the generalized burgers fluids. *Results Physics*, *7*, 4025–4032.

Krishna, Y. H., Reddy, G. V. R. & Makinde, O. D. (2018). Chemical reaction effect on mhd flow of casson fluid with porous stretching sheet. *Defect and Diffusion Forum*, *389*, 100–109.

Lund, L. A., Omar, Z., Khan, I., Baleanu, D. & Nisar, K. S. (2020). Dual similarity solutions of MHD stagnation point flow of casson fluid with effect of thermal radiation and viscous dissipation: stability analysis. *Scientific Reports*, *10*, 15405.

Maraj, E. N., Faizan, U. & Shaiq, S. (2019). Influence of joule heating and partial slip on casson nanofluid transport past a nonlinear stretching planar sheet. *Proceeding of the International Conference on Applied and Engineering Mathematics, ICAEM 2019*, 31–36.

Merkin , J. H. (1980). Mixed convection boundary layer flow on a vertical surface in a saturated porous medium. *Journal of Engineering Mathematics*, *14*(4), 301–313.

Mishra, G. S., Hussain, M. R., Seth, S. M. & Makinde, O. D. (2020). Stability analysis and dual multiple solutions of a hydromagnetic dissipative flow over a stretching / shrinking sheet. *Bulgarian Chemical Communications*, *52*(2), 259–271.

Najib, N., Bachok, N. & Arifin, N. M. (2017). Stability of dual solutions in boundary layer flow and heat transfer over an exponentially shrinking cylinder. *Indian Journal of Science and Technolology*, *9*(48).

Nandeppanavar, M. M., M. C., K. & Raveendra, N. (2021). Double-diffusive free convective flow of casson fluid due to a moving vertical plate with non-linear thermal radiation. *World Journal of Engineering, 18*(1), 85-93.

Oke, A. S., Mutuku, W. N., Kimathi, M. & Animasaun, I. L. (2020). Insight into the dynamics of non-newtonian casson fluid over a rotating non-uniform surface subject to coriolis force. *Nonlinear Engineering, 9*(1), 398-411.

Salleh, M. Z., Nazar, R. & Pop, I. (2010). Mixed convection boundary layer flow from a solid shpere with newtonian heating in a micropolar fluid. *SRX Physics*, *2010*, 736039.

Saidulu, N. & Lakshmi, A. V. (2017). MHD flow of casson fluid with slip effects over an exponentially porous stretching sheet in presence of thermal radiation, viscous dissipation and heat source/sink. *Asian Research Journal of Mathematics*, *2*, 1–15.

Salleh, S. N. A., Bachok , N., Arifin, N. M., Ali, F. M. & Pop, I. (2018). Stability analysis of mixed convection flow towards a moving thin needle in nanofluid. *Applied Sciences*, *8*(6).

Sarkar, T., Reza-E-Rabbi, S., Artifuzzaman, S. M., Ahmed, R., Khan, M. S. & Ahmmed, S. F. (2019). MHD radiative flow of Casson and Williamson nanofluids over an inclined cylindrical surface with chemical reaction effects. *International Journal of Heat and Technology*, *37*, 1117-1126.

Shah, Z., Kumam , P. & Deebani, W. (2020). Radiative MHD casson nanofluid flow with activation energy and chemical reaction over past nonlinearly stretching surface through entropy generation. *Scientific Reports*, *10*(1),1–14.

Shampine, L., Kierzenka , J. & Reichelt, M. (2000). Solving boundary value problems for ordinary differential equations in MATLAB with bvp4c. *Tutor Notes*, 75275, 1–27.

Tamoor, M., Waqas, M., Khan, M. I., Alsaedi, A. & Hayat, T. (2017). Magnetohydrodynamic flow of casson fluid over a stretching cylinder. *Results Physics*, *7*, 498–502.

Vaidya, H., Rajashekhar, C., Manjunatha, G., Prasad, K. V., Makinde, O. D. & Vajravelu K. (2020). Heat and mass transfer analysis of MHD peristaltic flow through a complaint porous channel with variable thermal conductivity. *Physica Scripta*, *95*(4).

W, P. D. & Awaludin, A. I. I. S. (2016). Stability analysis of stagnation-point flow over a stretching/shrinking sheet. *AIP ADVANCES*, 045308.

Zaib, A., Bhattacharyya, K., Uddin , M. S. & Shafie , S. (2016). Dual solutions of non-newtonian casson fluid flow and heat transfer over an exponentially permeable shrinking sheet with viscous dissipation. *Modelling and Simulation in Engineering*, 2016.

Zehra, I., Abbas, N., Amjad, M., Issakhov, A., Nadeem, S. & Saleem, S. (2021). Casson Nanoliquid flow with Cattaneo-Christov flux analysis over a curved stretching/shrinking channel. *Case Studies in Thermal Engineering*, *27*, 101146.